

Nitrogen evaluation in potato plants based on spectral data and on simulated bands of the VENμS satellite

Y. Cohen^{1*}, Y. Zusman^{1,2}, V. Alchanatis¹, Z. Dar³, D.J. Bonfil⁴, A. Karnieli⁵, A. Zilberman³, A. Moulin⁶, V. Ostrovsky¹, A. Levi¹, R. Brikman¹, and M. Shenker²

¹ *Agricultural Research Organization, Volcani center, Institute of Agricultural. Engineering, Bet-Dagan, Israel*

² *The Seagram Center for Soil and Water Sciences, Hebrew University of Jerusalem, Rehovot, Israel*

³ *Extension Service, The Ministry of Agriculture, Bet-Dagan, Israel.*

⁴ *Field Crops and Natural Resources Department, Agricultural Research Organization, Gilat Research Center, Israel.*

⁵ *The Remote Sensing Laboratory, Jacob Blaustein Institutes for Desert Research, Ben Gurion University of the Negev, Sede-Boker Campus, Israel.*

⁶ *Brandon Research Centre, Agriculture and Agri-Food Canada, Brandon, Manitoba, Canada*

*corresponding author: yafitush@volcani.agri.gov.il

Abstract

Five nitrogen (N) fertilization treatments were examined in potato fields in Israel in spring, 2006 and 2007, by measuring leaf spectral reflectance at 400-900 nm. The leaves were sampled and analyzed for petiole $\text{NO}_3\text{-N}$ and N percentage (leaf-%N). Leaf nitrogen content prediction models were developed based on Transformed Chlorophyll Absorption in Reflectance Index (TCARI) and Partial Least Square Regression (PLSR). Prediction models were also developed based on simulated bands of the future VEN μ S satellite. Spectral data correlated better with leaf-%N than with petiole $\text{NO}_3\text{-N}$. TCARI as a simple spectral index provided high correlations with leaf-%N, but was limited to the tuber-bulking stage. PLSR analysis gave better correlation than TCARI with leaf-%N. An R^2 of 0.95 ($p < 0.01$) and overall accuracy of 80.5% (kappa = 74%) were determined for both vegetative and tuber-bulking periods. The simulated VEN μ S bands gave similar correlation with leaf-%N to that of the spectrometer spectra. The satellite has significant potential for spatial analysis of nitrogen level through inexpensive very-wide-area images every 2 days.

Keywords: Spectral data; VEN μ S satellite; TCARI; PLSR; Nitrogen; Potato.

Introduction

Potato is an important crop worldwide, with total world production of about 360 million metric tons (National Potato Council [NPC] 2006). Potato is becoming a very important crop also in Israel: in 2000 an area of 11,000 ha was seeded, which in 2005 had increased

to around 17,000 ha (<http://www.cbs.gov.il/reader/>). Potato yield and quality are highly dependent on an adequate supply of nitrogen (Dar, 2002; Errebhi et al. 1998). The relatively shallow root system of the potato crop, coupled with its nitrogen (N) requirement and sensitivity to water stress on coarse textured soils increases the risk of nitrate ($\text{NO}_3\text{-N}$) leaching. Therefore, precise N management for potato (*Solanum tuberosum* L.) is important, both for maximizing production and for minimizing N loss to groundwater. Applying the right amount of N in the right place at the right physiological stage presents a challenge to potato growers, and matching fertilizer supply to the demands of the crop requires an adequate assessment of N status in the field. Potato growers usually apply safety factors to increase fertilization levels beyond the recommendations, in response to uncertainties regarding the accuracy of the recommendations, because growers do not want to sacrifice high-value yield and because there are few commercially available sensors to assess N status (Shock et al., 2007; Zebarth and Rosen, 2007) or that account for spatial variability. The recent significant increase in fertilization costs has prompted efforts to devise strategies that will improve N use efficiency (NUE) in the major crops such as potato. Previous research concluded that split application of N to match potato growth needs would significantly improve NUE (e.g., Westermann and Kleinkopf, 1985). Potatoes are grown under irrigation, primarily on coarse, low-organic-content, sandy soils that are subject to nitrogen (N) leaching when water and N are applied in excess (Alva 2008). Errebhi et al. (1998) showed that N management that reduced the amounts of N applied at planting resulted in lower $\text{NO}_3\text{-N}$

leaching, higher N recovery by the crops, and improved yield of marketable tubers. Meyer and Marcum (1998) demonstrated the need for pre-planting measurements of soil-N concentration for determining appropriate applied N rates, and Dar (2002) suggested that the appropriate mid-season N rates and timing of application might be determined from petiole $\text{NO}_3\text{-N}$ concentrations. Because of the temporal variability of soil N supply, strategies based on detecting crop N status at critical crop growth stages, and meeting crop N requirements with carefully timed fertilization may ultimately be more successful in improving NUE than those based on application at planting (Ferguson et al. 2002; Van-Alphen and Stoorvogel 2000). However, fertilizer management in irrigated potato production is currently based on uniform N application rates and does not account for spatial variability of plant N demand, which may result from in-field variability of soil and environmental characteristics. In the light of these considerations, there is considerable potential for varying the recommended N-application timing and rates according to petiole N level as determined by space-based measurements of soil and crop properties at critical points of the growing season.

Remote sensing techniques can indicate crop N status (Al-Abbas et al. 1974; Botha et al. 2006; Gitelson et al. 2003; Jain et al. 2007; Thomas and Gausman 1977; Zakaluk and Ranjan 2007). Light reflected by vegetation in the visible region of the spectrum is predominantly influenced by the presence of chlorophyll pigments in the leaf tissues, and these relate to the leaf N concentration (Haboudane et al., 2002). Chlorophyll a and b absorb light in the red (~ 670 nm) and blue (~ 450 nm) portions of the spectrum (Gates et

al. 1965), thereby providing diagnostic absorption features. Additionally, near-infrared (NIR) reflectance is influenced by the internal leaf cell structure: well hydrated, healthy, spongy mesophyll cells strongly reflect infrared wavelengths (Gates et al., 1965). The spectral region between the red absorption feature and the region of high NIR reflectance, termed the "red-edge", changes shape and position when the plant enters N deficiency (Jain et al. 2007; Strachan et al. 2002). Therefore, measurements of reflected energy from crop leaves and canopies can be used to rapidly estimate chlorophyll concentration and, thereby, to provide a measure of N content (Haboudane et al. 2002; Jain et al. 2007).

The use of hyperspectral (HS) images, validated by ground based sensors of spectral reflectance, can be used to address both spatial and temporal variability of leaf N content in order to improve mid-season N management. HS images obtained by the Hyperion Satellite combine high spectral resolution on one hand, but with moderate spatial and temporal resolutions on the other hand. In 2009, the VEN μ S satellite is to be launched (<http://smc.cnes.fr/VENμS>). VEN μ S is a research joint mission of the French Centre National d'Etudes Spatiales (CNES) and the Israel Space Agency (ISA). The system has spectral, spatial and temporal resolutions suitable for precision agriculture (PA), i.e. 12 narrow spectral bands (16–40 nm full width at half maximum, FWHM) in the visible and NIR ranges (420–910 nm); ground resolution of 5.3 m, and a 2-day revisit time. The seven bands of the multi-spectral mode of the Compact Airborne Spectrographic Imager (CASI) are similar to some of the VEN μ S bands. Three of the CASI bands were successfully used to estimate chlorophyll content and to discriminate between N treatments in corn fields in

Canada (Haboudane et al. 2002). Moreover, thanks to the unique combination of high spectral, spatial and temporal resolutions, and free availability of data during the first 2-4 years of operation, it is expected to stimulate the adoption of PA concepts in large areas, in conjunction with research in a variety of environmental conditions. The present paper describes part of an ongoing research project that aims to assess the potential of state-of-the-art super-spectral (SS) and HS imaging technology for delineating management zones (MZ) for variable-rate N application on potatoes. The objective of this study was to determine the relationships between spectral data and simulated bands of the VENμS satellite, and nitrogen levels in potato petioles and leaves.

Materials and methods

The study was conducted in the spring growing seasons of 2006 and 2007, on two commercial potato (*Solanum tuberosum* L.) (*Solanaceae*) fields planted with cv. Desiree in Kibbutz Ruhama, Israel (31.38° N, 34.59° E). This agricultural land lies in the southern part of Israel's coastal plain, on the boundary between Mediterranean and semi-arid climates. The soil type of both fields is sandy loam. The two fields follow a potato-wheat-sunflower/chickpea-wheat-potato crop rotation. Potato seed tubers were planted such that hills (i.e., pairs of rows) were spaced 1.93 m apart, with a within-row spacing between plants of 0.2 m. The plots were planted at the beginning of February and harvested in mid-June. The average temperatures during this period range between 15° and 35°C. The average annual rainfall during the spring season in this region is 100 mm. In both seasons

the plots received the same applications of pre-season compost ($30 \text{ m}^3 \text{ ha}^{-1}$), phosphate (180 kg ha^{-1}) and KCl (180 kg ha^{-1}).

In order to assess the N status of potatoes, five N treatments with four replicates were applied in each season. In 2006 an area of 1.2 ha was divided into 20 sub-plots with dimensions of 5 X 120 m. In 2007, in order to enable the recognition and analysis of the sub-plots in airborne hyper-spectral images, an area of 8 ha was divided into sub-plots with dimensions of 18 X 50-100 m. The treatments in both seasons included commercial treatment (fertigation) with N (urea) at 400 kg ha^{-1} and application of Multigro 43-0-0 SRN, a coated urea granular slow-release fertilizer (Haifa Chemicals Inc., Haifa, Israel) applied at N rates ranging from 0 to 335 kg ha^{-1} before planting (Tables 1 and 2).

Table 1: N treatments applied in the potato field in spring 2006

ID	N rate (kg ha^{-1})	N rate relative to commercial rate	Application type
T100%	400	100%	Commercial (urea); fertigation
T84%	335	84%	Multigro® 43-0-0 SRN
T54%	215	54%	Multigro® 43-0-0 SRN
T25%	100	25%	Multigro® 43-0-0 SRN
T0%	0	0	

Table 2: N treatments applied in the potato field in spring 2007

ID	N rate (kg ha ⁻¹)	N rate relative to commercial rate	Application type
T100%	400	100%	Commercial (urea); fertigation
T75%	300	75%	Multigro® 43-0-0 SRN
T50%	200	50%	Multigro® 43-0-0 SRN
T25%	100	25%	Multigro® 43-0-0 SRN
T0%	0	0	

Spectral data collection

Reflectance of leaves in the field was measured with an HR2000 mini-spectrometer (OceanOptics Inc., Dunedin, FL, USA) with a spectral range of 400-900 nm and a 50- μ m slit. The optical spectral resolution of the system, determined by the slit width and the diffraction grating, was 1.8 nm (FWHM). The spectrometer was equipped with a 2048-pixel CCD array, with signal-to-noise ratio of 250:1, connected to a laptop computer through a USB port. An LS-1 halogen light source (Ocean Optics), in combination with a fiber optic reflectance probe were used to illuminate the leaf and to collect the reflected light. The reflectance probe consisted of six 400- μ m-diameter optical fibers arranged in a circle to illuminate the sample, and a sensing fiber which transferred the reflected light to the spectrometer. A sampling cell was designed and constructed for in-field leaf-reflectance measurements. The sampling cell shielded the sampled leaf against ambient light, and maintained a constant distance of 10 mm between the leaf sample and the reflection probe (Alchanatis et al. 2005). Integration time was 1500 ms, with an average of

three spectra per acquisition. White and dark reference signals were sampled at the beginning of each plot.

Field observations were conducted on four cloudless days in each of the two seasons. On each day, spectral reflectance was measured in the youngest fully expanded leaf of each of 20 plants from each of the two replicates of each N treatment. These leaves were sampled and $\text{NO}_3\text{-N}$ was measured in five 4-petiole groups for each of the sampled sub-plots. In 2007 leaves were analyzed for leaf-%N also.

The spectral data from the second acquisition date in 2006 were found to be corrupted and were not used for further analysis. Table 3 summarizes the measurement dates and the available spectral and ground truth data.

Table 3: Summary of measurement dates and available spectral and ground truth data

	Days after planting	Spectral measurements	Petiole $\text{NO}_3\text{-N}$ analysis	Total %N in leaves
2006	50	√	√	Not measured
	78	corrupted	√	Not measured
	92	√	√	Not measured
	99	√	√	Not measured
2007	55	√	√	√
	69	√	√	√
	82	√	√	√
	97	√	√	√

Spectral data analysis

Prediction models of N levels were developed by means of three analytical methods: 1. TCARI calculation; 2. Partial Least Square Regression (PLSR) analysis of the whole spectrum; and 3. Simulation of the VENμS bands, followed by TCARI calculation, and multivariate linear regression analysis of the simulated bands.

TCARI calculation. Transformed Chlorophyll Absorption in Reflectance Index (TCARI), following Haboudane et al. (2002), was calculated for means of replication results according to Equation 1:

$$TCARI = 3[(\rho_{700} - \rho_{670}) - 0.2(\rho_{700} - \rho_{550})\left(\frac{\rho_{700}}{\rho_{670}}\right)] \quad (1)$$

The TCARI is a modification of the Modified Chlorophyll Absorption in Reflectance Index (MCARI) that was developed by Daughtry et al. (2000):

$$MCARI = [(\rho_{700} - \rho_{670}) - 0.2(\rho_{700} - \rho_{550})\left(\frac{\rho_{700}}{\rho_{670}}\right)] \quad (2)$$

According to Gitelson and Merzlyak (1998), wavelengths in the range 530-630 nm, and of 700 nm are sensitive to chlorophyll content in plant leaves. The 550-nm band matches the minimum chlorophyll absorption in the VIS region (Haboudane et al. 2002), therefore the MCARI is composed of one chlorophyll absorption band at 670 nm, and two chlorophyll-sensitive bands, 550 and 700 nm. The MCARI was applied for corn (Daughtry et al. 2000; Haboudane et al. 2002, 2004), wheat, and soybean (Haboudane et al. 2004).

The TCARI is calculated from the same bands as the MCARI, but the ratio between the reflectance at 700 and 670 nm is used to filter the background reflectance at 700 and 550 nm. Hu et al. (2004) successfully predicted chlorophyll content from airborne sensor measurements by applying TCARI/OSAVI to corn, soybean, and wheat fields. Zarco-Tejada et al. (2005) compared vine chlorophyll estimations obtained with TCARI and with TCARI/OSAVI, and found TCARI advantageous for pure vegetation data, and TCARI/OSAVI for mixed soil and vegetation data. When applied to the potato canopy level TCARI was found insensitive to changes in N content (Jain et al. 2007); this might have been because the TCARI was not normalized by the OSAVI.

In the present study a regression model that linked the means of replicate data of TCARI and leaf N levels was calculated for 66% of the data. The regression model was applied to the entire data set when the Pearson correlation statistic, R , was statistically significant ($p < 0.05$).

PLSR analysis. Partial Least Square Regression (PLSR) analysis is a chemometric technique that generalizes and combines the methods of Principal Component Analysis (PCA) and multiple regressions; it is used to predict a set of dependent variables from a large set of independent ones (i.e., predictors) that may be correlated. PLS Analysis enabled the prediction of N status in wheat and corn from ground-based spectral data (Alchanatis et al. 2005; Bonfil et al., 2005) and in forests from hyperspectral images (Coops et al. 2003; Ollinger et al. 2002; Smith et al. 2002; Townsend et al. 2003). PLS analysis of spectra is based on statistical analysis of wavelengths from a wide spectrum, in contrast to linear

regression for indices such as TCARI; it exploits the high dimensionality of the spectral data by building predictive models based on a few extracted factors, also called components or latent variables (LVs), with the constituent concentration data (e.g., N concentration) used directly during the spectral decomposition process (Shenk and Westerhaus, 1991). As a result, full-spectrum wavelength loadings for significant PLS factors, from which regression coefficients are derived, are directly related to concentrations of constituents, and therefore describe the spectral variation most relevant to the modeling of chemical variations. In the present study, the independent variables for the PLS analysis were the raw spectra and the first-derivatives of the reflectance spectra over the whole measured range (400-900 nm). They were used to predict both Petiole $\text{NO}_3\text{-N}$ and leaf-%N. In contrast to the TCARI analysis, which was based on means of replicate data, in the PLSR analysis all data from all sites were used as input. Thus, for petiole $\text{NO}_3\text{-N}$ there were 350 samples (50 from each of seven dates), and for leaf-%N there were 200 samples (50 from each of four dates) (Table 3). The first derivative was calculated for a given wavelength as the difference in smoothed reflectance (Savgol smoothing, 15-nm average). The use of first-derivative spectra provided a surrogate for identifying the actual absorbance features that form the physical basis for identifying N concentration through spectroscopy. Specifically, the first-derivative identifies differences between the slopes of the spectra, meaning that absorbance features related to canopy chemistry are identified through relative differences in the linear rate of change of reflectance within a given wavelength region. As a consequence,

the actual bands identified as being related to N concentration may not, in fact, be centered on wavelengths known to exhibit absorbance features, but rather on those adjacent to known absorbance features. In addition, the use of the first derivative enables baseline offsets and low-frequency variations to be removed or substantially minimized (Smith et al. 2002). For our present application, the performances of the models were evaluated by using leave-one-out cross validation. The PLSR models were calibrated and cross validated with the PLS Toolbox (Eigenvector Research Inc., Wenatchee, WA, USA) and MATLAB software (The MathWorks, Natick, MA, USA). The number of latent variables for each model was selected by choosing the number that yielded the lowest Root Mean Square Error of Cross Validation (RMSECV). The measured and the predicted N values were then averaged for each replication and the Standard Error of Prediction (SEP) in the cross-validation process was used as an indication of the average model error.

Simulation of VEN μ S satellite bands, TCARI calculation, and MLR analysis. Based on the spectrometer data, we simulated 10 out of 11 VEN μ S bands (Table 4), taking into account the equivalent central wavelength (nm) and the FWHM. The theoretical spectral response of each VEN μ S band was overlaid with the actual spectral reflectance curve obtained from the spectrometer. The TCARI was calculated based on equation 1 where bands 550, 670, and 700 nm were shifted with the simulated VEN μ S bands 555, 672, and 702, respectively. Since there is a small number of VEN μ S bands, Multivariate Linear Regression (MLR) analysis and not the PLSR was applied, based on 10 simulated VEN μ S bands. The MLR was

applied to data from all sites from all dates. The measured and the predicted N values were then averaged for each replication and the SEP in the cross-validation process was used as an indication of the average model error.

Table 4: VEN μ S spectral bands

Band number	Equivalent central wavelength (nm)	FWHM ¹ (nm)	Region
1	420	40	Blue
2	443	40	Blue
3	490	20	Green
4	555	20	Green
5-6	638	24	Red
7	672	16	Red edge
8	702	16	Red edge
9	742	16	Red edge
10	782	16	NIR
11	865	20	NIR
12*	910	20	NIR

*Band 12 was not simulated, since the spectral range measured was 400-900 nm.

Evaluation of model performance

Accuracy of the prediction models was evaluated by means of the coefficient of determination (R^2) and the Root Mean Square Error (RMSE). Classification accuracy was determined with the Kappa coefficient for four classes of measured and predicted petiole $\text{NO}_3\text{-N}$ and leaf-%N values, which represented a reasonable number of possible variable application rates. The classes were based on intervals of 250 ppm and 0.5% for petiole $\text{NO}_3\text{-N}$ and leaf-%N, respectively (Table 5).

Table 5: Petiole NO₃-N and leaf-%N classes

N level	Petiole NO ₃ -N range	Leaf-%N range
1	< 250 ppm	< 3.5%
2	250-500 ppm	3.5-4.0%
3	500-750 ppm	4/0-4.5%
4	> 750 ppm	4.5-5.0%

A confusion matrix was determined in order to calculate the KAPPA coefficient of agreement for each model in which the principal diagonal entries reflected the correct classification. The proportion of the total number of correctly classified instances among the total number of instances represented the “overall accuracy” of the classification. Based on overall and chance accuracy (proportion of units expected for chance agreement) the KAPPA coefficient of agreement (K) was calculated with equation 3 (Tso and Mather 2001):

$$k = \frac{N \sum_{i=1}^r X_{ii} - \sum_{i=1}^r (x_{i+} \times x_{+i})}{N^2 - \sum_{i=1}^r (x_{i+} \times x_{+i})} \quad (3)$$

where r is the number of rows in the confusion matrix; x_{ii} is the number of combinations along the principal diagonal; x_{i+} is the total number of observations in row i; x_{+i} is the total number of observations in column i; and N is the total number of instances. In addition,

the percentages of erroneous classification of instances to adjacent classes on two or three levels of proximity, i.e., high-cost errors, were calculated.

Results

Temporal changes in N levels and yield variables

Petiole $\text{NO}_3\text{-N}$ decreased during the growing season in all fertilizer treatments. When petiole $\text{NO}_3\text{-N}$ data for day 50 after planting in 2006 were compared with optimal, excess, and deficient guidelines (Dar, 2002) (Fig. 1a), means for all treatments were close to the optimum value, with the exception of the 'no-N' treatment (T0%). On all other days, petiole $\text{NO}_3\text{-N}$ levels of T100%, T84%, and T54% were above the excess guideline, while the T25% and T0% were below the deficit.

The 2007 data (Fig. 1b) show that similar temporal changes occurred, with a few differences. Whereas T100% and T75% values were close to the optimum guideline or above the excess at all dates, those in T25% and T0% were close to or below the deficit borderline. Petiole $\text{NO}_3\text{-N}$ concentrations for T50% were close to the optimal level on the first three dates, but were below the deficit borderline on the last date, i.e., 97 days after planting, and those for T25% and T0% behaved similarly.

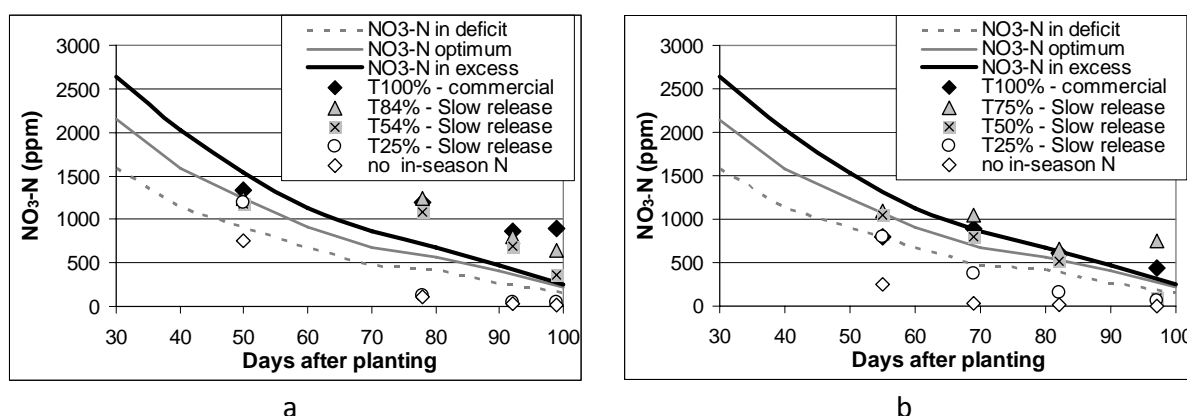


Figure 1: Optimal, excess, and deficit guidelines for petiole $\text{NO}_3\text{-N}$ in potato, 'Desiree', for the spring season versus petiole $\text{NO}_3\text{-N}$ levels found in each treatment on each date in 2006 (a) and in 2007 (b)

Potato yield and quality were assessed for each treatment in each year of the study (Fig. 2). With the slow-release formulations, yield quantity and quality increased with increasing N content, and reached maximum values at a fertilization rate of around 50%, with no significant differences ($p < 0.05$) from the values in T84% in 2006 and T75% in 2007. Nevertheless, both yield variables were slightly lower in T84% than in T54% in 2006, whereas in 2007 those in T75% were slightly higher than those in the latter two. The commercial fertigation treatment, T100%, elicited different responses in each season: in 2006 its values were similar to those in T54% and higher than those in T84%, whereas in 2007 T100% gave lower values than either T50% or T75%.

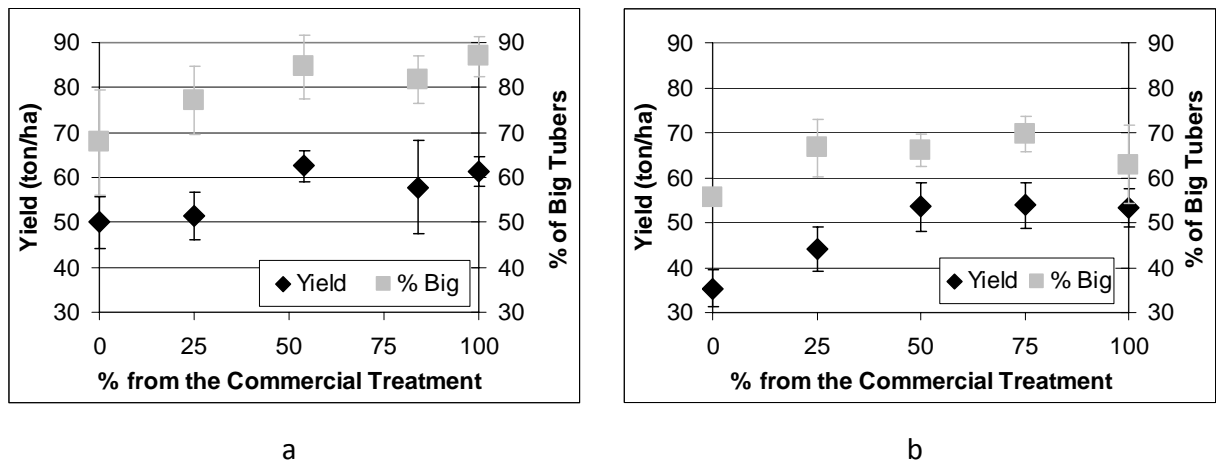


Figure 2: Yield quantity and quality in each treatment in 2006 (a) and in 2007 (b).

Bars represent ± 1 STD values

Relationships between TCARI and N levels

Petiole $\text{NO}_3\text{-N}$ content, leaf-%N and TCARI values were averaged among replicates. All petiole $\text{NO}_3\text{-N}$ contents from all dates in the two spring seasons were plotted against TCARI values (Fig. 3). In the case of the 'TCARI - $\text{NO}_3\text{-N}$ ' relationships the data from 50-55 days after planting, i.e., the end of the vegetative growth period, differed from the data from the tuber-bulking period, i.e., from 60 to 100 days after planting. For the first period, there were different negative linear models for each season. From 70 days after planting a single negative non-linear relationship was found between TCARI and petiole $\text{NO}_3\text{-N}$ content for both seasons. The RMSECV was 326 ppm, which is around 30% of the range of petiole $\text{NO}_3\text{-N}$ content (0-1100 ppm). Moreover, the non-linear model provided a qualitative separation between the two main levels of petiole $\text{NO}_3\text{-N}$ content, i.e., lower and higher than 250 ppm. This binary division exhibited an overall accuracy of 90% ($n =$

41). The confusion matrix for four groups is presented in Table 6. It can be seen that when the $\text{NO}_3\text{-N}$ content was classified into four levels the overall accuracy was reduced to 61% ($p < 0.01$) with Kappa of 41.5%. In addition, there were 19.5% ($n = 8$) of high-cost errors.

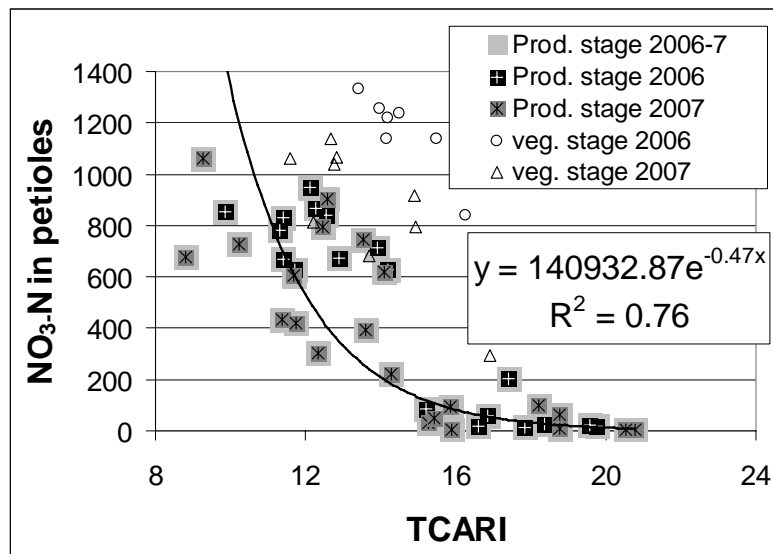


Figure 3: $\text{NO}_3\text{-N}$ as a function of TCARI values from all term dates in both seasons

Table 6: Confusion matrix between measured and predicted petiole $\text{NO}_3\text{-N}$ values, based on TCARI model

		Predicted petiole $\text{NO}_3\text{-N}$ (ppm)				Overall accuracy 25/41=61% high cost errors (in gray): 8/41=19.5%
		<250	250-500	500-750	>750	
Measured petiole $\text{NO}_3\text{-N}$ (ppm)	<250	19				
	250-500	1	1	2		
	500-750	3	2	3	1	
	>750		5	2	2	

A better correlation was found between TCARI and leaf-%N for the 2007 data. Figure 4a shows that, when data from the first term date were excluded, a negative linear relationship was found between TCARI and leaf-%N. For comparison, Fig. 4b presents the scatter plot of TCARI against $\text{NO}_3\text{-N}$ from 2007. The RMSE of 'TCARI - leaf-%N' was 0.2% which is 10% of the range of leaf-%N (2.9-4.8%). The overall accuracy and kappa coefficient were 81% ($p < 0.01$) and 72.5%, respectively, with no high-cost errors ($n = 26$).

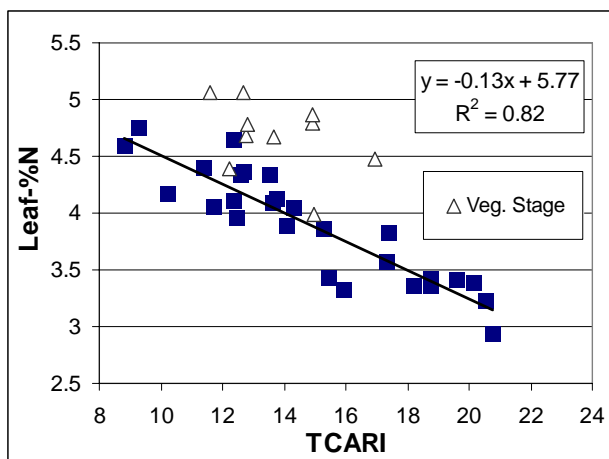


Figure 4a: Leaf-%N as a function of TCARI values for all sampling dates in 2007

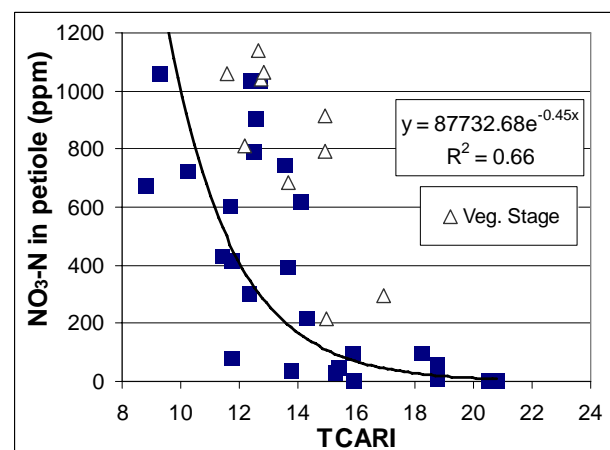


Figure 4b: Petiole $\text{NO}_3\text{-N}$ as a function of TCARI values for all sampling dates in 2007

Partial least square regression (PLSR) analysis

Prediction models were developed by applying PLSR analysis to the raw reflectance and to their first derivative, and both yielded similar results. The PLSR analysis yielded prediction models of petiole $\text{NO}_3\text{-N}$ with $R^2 = 0.82$ ($n = 64$; $p < 0.01$) for all data from all dates in both

seasons (Fig. 5a). The best prediction model for reflectance was determined with 10 latent variables (factors), and the first derivative was calculated with only five. The RMSECVs of both models were 164 ppm, or 12% of the range of petiole $\text{NO}_3\text{-N}$ content (0-1100 ppm). This is an improvement of 50% over the TCARI-based model. The overall classification accuracy for four groups and the Kappa coefficient were 70 and 59%, respectively, with no high-cost errors.

The correlation between spectral data and leaf-%N values for the model developed with PLSR was much higher (Fig. 5b; $R^2 = 0.95$, $n = 36$; $p > 0.01$). The RMSECV was 0.11%, i.e., 5% of the range of leaf-%N values (2.9-5.1%). Overall classification accuracy and Kappa coefficient were 80.5 and 74%, respectively, with no high-cost errors.

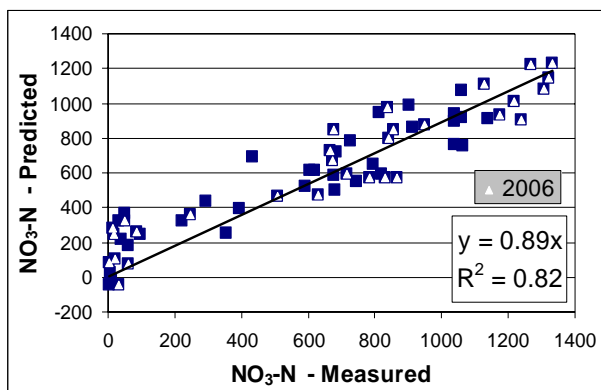


Figure 5a: Measured against predicted petiole $\text{NO}_3\text{-N}$ contents from all term dates in 2006-7, based on PLSR analysis

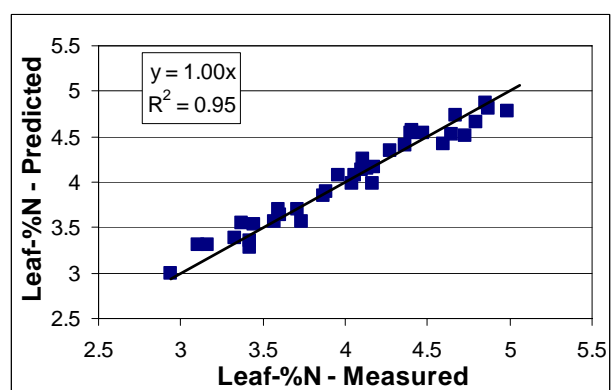


Figure 5b: Measured against predicted leaf-%N values from all term dates in 2007, based on PLSR analysis

Analysis of simulated VEN μ S bands

The petiole NO₃-N and leaf-%N were analyzed by using TCARI as calculated from three of the simulated VEN μ S bands, and also by multiple linear regression (MLR) applied to all spectra. The relationships between TCARI based on the VEN μ S simulated bands and petiole NO₃-N and leaf-%N (Figs 6a and 6b) were similar to their equivalents based on the original narrow bands of the spectrometer data (Figs 4a and 4b). The relationship between TCARI and leaf-%N was similar ($R^2 = 0.81$; $n = 27$; $p < 0.01$; RMSE 9%), but lower accuracy was found when four classes were used (overall accuracy of 67% and kappa of 53%).

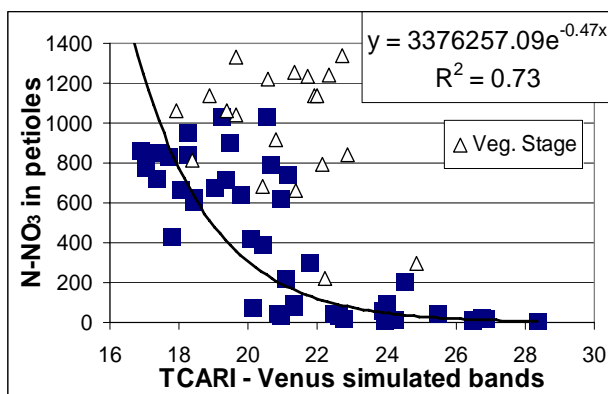


Figure 6a: Petiole NO₃-N as a function of TCARI values using the simulated VEN μ S bands for all sampling dates in 2006-7

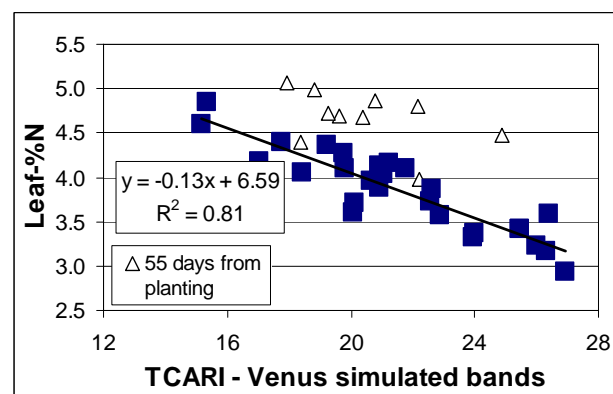


Figure 6b: leaf-%N as a function of TCARI values using the simulated VEN μ S bands for all sampling dates in 2007

MLR models, calculated with the simulated VEN μ S bands yielded inferior results to those of similar models based on the original spectral data. The correlation with petiole NO₃-N content was low ($R^2 = 0.46$; $n = 64$), with an RMSE of 233.8 ppm (17.5% of the

overall range; Fig. 7a). Furthermore, the accuracy of the overall petiole $\text{NO}_3\text{-N}$ classification, and the kappa coefficient were only 56 and 40%, respectively, with 2% of high-cost errors.

In contrast, leaf-%N was highly correlated with the simulated bands (RMSECV = 0.19%, 9% of the overall range; Fig. 7b). However, the overall classification accuracy and kappa coefficient were 66 and 53%, respectively, with no high-cost errors.

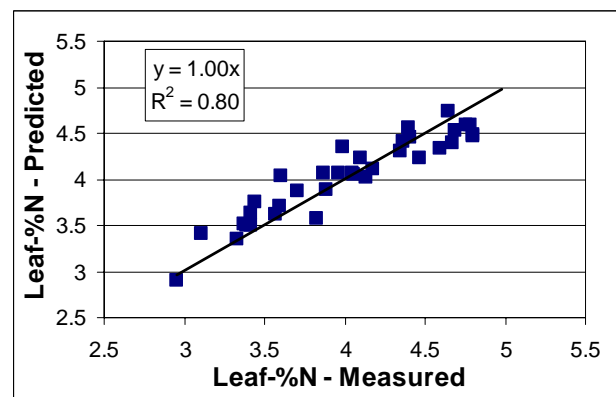
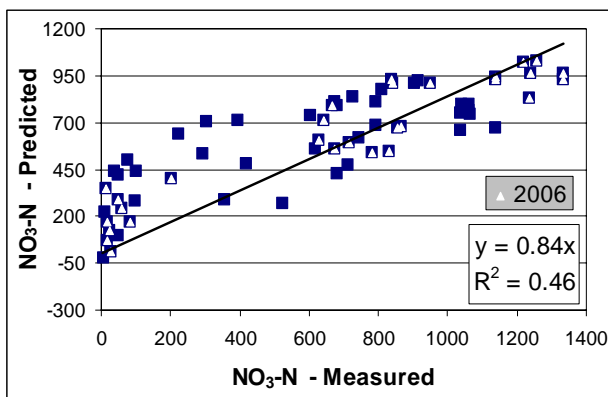


Figure 7a: Measured against predicted petiole $\text{NO}_3\text{-N}$ content from all term dates in 2006-7, based on MLR analysis of the simulated VEN μS bands

Figure 7b: Measured against predicted total %N from all term dates in 2007, based on MLR analysis of the simulated VEN μS bands

Discussion

Table 6 summarizes the performance measures of all analysis types. Leaf-%N was better correlated with spectral data than petiole $\text{NO}_3\text{-N}$. This may be attributed to the fact that petiole $\text{NO}_3\text{-N}$ reflects N status in the short term whereas leaf-%N represents it in the

longer term. The TCARI was reasonably correlated with leaf-%N, but was limited to the tuber-bulking stage. The use of the full measured spectrum (400-900 nm) with PLSR analysis increased the accuracy of estimates of N levels compared with use of a few selected bands and the index calculation of TCARI. In addition and in contrast to the TCARI results, a single model was found to apply to both the vegetative and the tuber-bulking periods. Furthermore, PLSR analysis achieved better accuracy in terms of all performance measures.

Table 6: Accuracy indices for the various types of data analyses

Data type	Nitrogen index (Season)	Analyses technique	R ²	RMSE (%)	Overall accuracy	Kappa	High-cost errors	Phenological stage
Original spectra	Petiole NO ₃ -N content 2006-7	TCARI	0.76* n=41	30%	61%	41.5%	19.5%	TuberBulk
		PLS	0.82* n=65	12%	70%	59%	0%	Veg. + TuberBulk
	Leaf-%N - 2007	TCARI	0.80* n=26	10%	81%	72.5%	0%	TuberBulk
		PLS	0.95* n=36	5%	80.5%	74%	0%	Veg. + TuberBulk
Simulated VEN μ S bands	Petiole NO ₃ -N content 2006-7	TCARI	0.73* n=44	27%	64%	45%	9%	TuberBulk
		MLR	0.46* n=64	18%	56%	40%	2%	Veg. + TuberBulk
	Leaf-%N - 2007	TCARI	0.81* n=27	9%	67%	53%	0%	TuberBulk
		MLR	0.80 n=35	9%	66%	53%	0%	Veg. + TuberBulk

PLS vs TCARI

The relative importance of spectral wavelengths can be determined with the PLSR analysis. The relative importance of each wavelength can be evaluated according to the Variable Importance in Projection (VIP) of the independent variables. In general, a VIP value higher than one unit indicates that the contribution of that wavelength is significant, and the higher the VIP value, the greater the contribution of that wavelength to the model. Despite the differences between the VIP values obtained by PLSR analysis of the raw reflectance data (Fig. 8a) and of the first derivatives (Fig. 8b), two expected ranges can be observed: 450-530 nm and 680-730 nm. The first range features rapid change from relatively low reflectance in the blue range to higher reflectance in the green range (Fig. 8c); the second range straddles the red edge (Fig. 8c). The spectra in the 450–530 nm range are strongly influenced by the presence and abundance of chlorophyll a and b (Gates et al. 1965; Townsend et al. 2003). In contrast, the spectra in the 680-730 nm range may be correlated with leaf area index also. In the relatively limited spectral range measured in the present study, (in contrast to the SWIR), these were the spectrum ranges that could be indirectly related to nitrogen content. These results are consistent with those of studies that analyzed hyperspectral images with PLSR for estimating N concentrations in forests (Coops et al. 2003; Smith et al. 2002).

Within these two ranges high VIP scores (of the raw spectra and the first derivative) were obtained for the TCARI bands. Yet, the high VIP scores for a wider range around these bands showed the importance of the gradual change in reflectance for

prediction of leaf-%N. Thereby, the predictive potential of PLSR analyses of spectra is higher than that for indices like the TCARI.

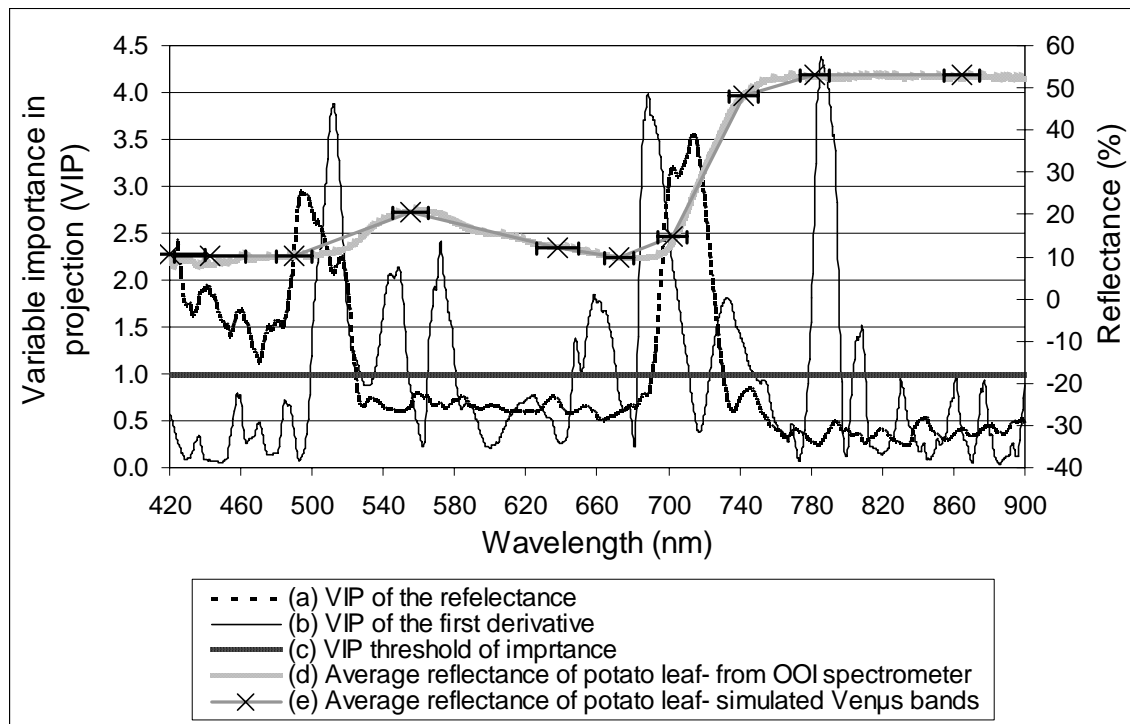


Figure 8: VIP of the PLS models based on the reflectance (a) and the first derivative (b). VIP threshold of significant importance (c). Average reflectance of a potato leaf based on the original spectra (d) and on VEN μ S simulated bands (e). The horizontal bars represent the FWHM of the VEN μ S bands.

Spectrometer reflectance vs. simulated VEN μ S bands:

The simulated VEN μ S bands performed similarly to the measured spectra, with regard to the prediction of leaf-%N. However, the accuracy was much lower for prediction of petiole NO₃-N content. Seven of the 11 simulated VEN μ S bands were located in the two

important transition zones (Table 4), a distribution that enables their use for evaluating leaf-%N. However, because of the far fewer bands and their greater width (Fig. 8e) the VEN μ S bands may acquire a significant part of the differences in the transitions but their use may not be as accurate as the use of the intensive spectral data.

TCARI. Comparison of two TCARI-based models for prediction of leaf-%N – a comparison via the intensive spectral data of the spectrometer (Fig. 4a) and via the simulated VEN μ S bands (Fig. 6b) – shows the importance of the wavelengths and distribution of the VEN μ S bands. The two models have identical slopes (-0.13) but different intercepts. This is attributed to a shift of the TCARI values when they are calculated for the simulated VEN μ S bands (Fig. 9). Thereby, despite the expected high correlation between the two sets of TCARI values (Fig 9), the TCARI values derived from the simulated VEN μ S bands are significantly ($p < 0.001$) higher than those based on the original spectral data. The 550- and 700-nm bands of the TCARI are located on transition zones of typical leaf spectra (Fig. 8d,e), and the equivalent VEN μ S bands for TCARI are not identical to the original central bands, as suggested by Haboudane et al. (2002) (Equation 1, Table 4). Also, the VEN μ S bands are much wider than the spectrometer ones. Both modifications especially in transition zones contribute to the differences in reflectance of the TCARI bands especially in the red-edge range (Figure 10). These differences resulted in significantly different TCARI values, which altered the prediction model intercept.

MLR analysis. When all simulated VEN μ S bands are analyzed by the MLR method these differences in reflectance may be enhanced, as can be seen in the results derived from

the PLSR models of the intensive spectral data and the MLR models of the simulated VEN μ S bands, and their accuracies (Table 6; Figs 5 and 7).

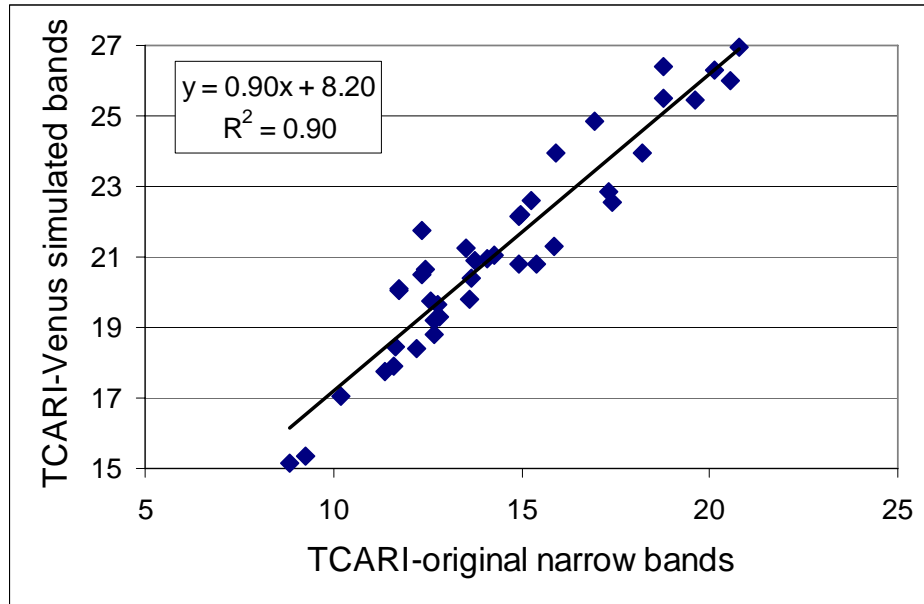


Figure 9: TCARI based on the original narrow bands against TCARI based on the simulated VEN μ S bands (data from 2007)

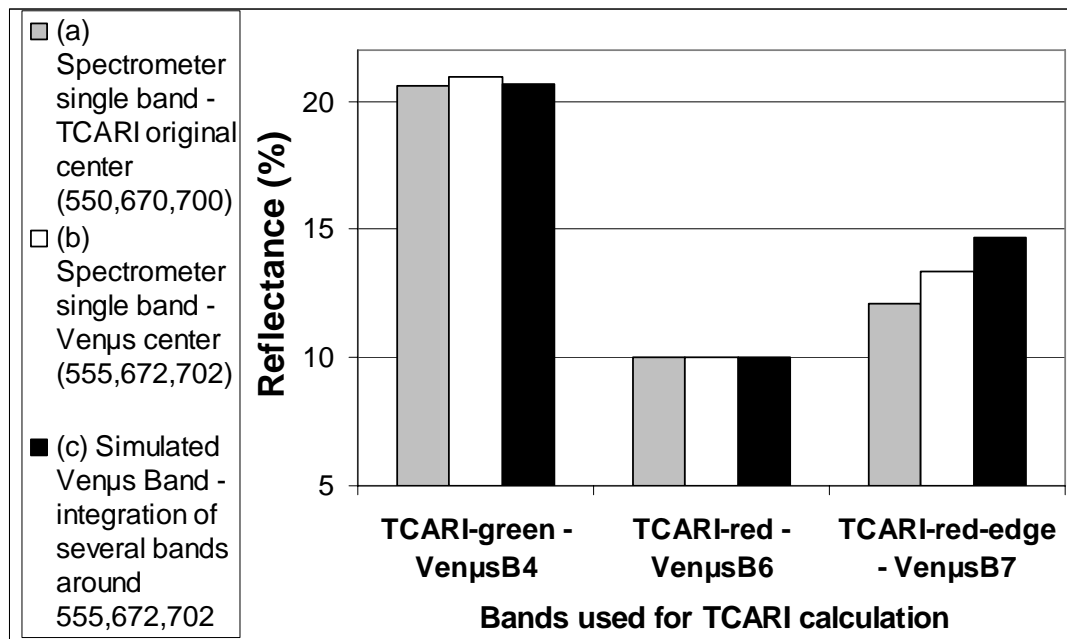


Figure 10: Reflectance of original TCARI bands from the spectrometer (a) and as related to the center (b) and width (c) of the simulated VENµS bands.

Summary and Conclusions

The results of this study demonstrate the potential of few spectral indices and sensors for temporal monitoring of nitrogen levels in potato fields. The TCARI for single leaves in the field was significantly correlated with potato petiole $\text{NO}_3\text{-N}$ and leaf-%N. A model based on PLSR of the spectrum in the 400-900 nm range was highly correlated with petiole $\text{NO}_3\text{-N}$ and leaf-%N during the vegetative and tuber-bulking periods. The correlation of simulated VENµS spectra with leaf-%N was similar to that of the spectra obtained from the spectrometer. However, the correlation was weaker with respect to petiole $\text{NO}_3\text{-N}$. The VENµS satellite has considerable potential for spatial analysis of leaf-%N since it can

provide images of very wide areas every 2 days at low cost. However, in Israel (and also in other countries, e.g., the USA and Canada) decisions on fertilization of potato fields in the course of the season are based on petiole sampling and chemical analysis for $\text{NO}_3\text{-N}$ content, which is relatively quick and cheap. The 2007 data show that the correlation between petiole $\text{NO}_3\text{-N}$ and leaf-%N was statistically significant but low (Fig. 11).

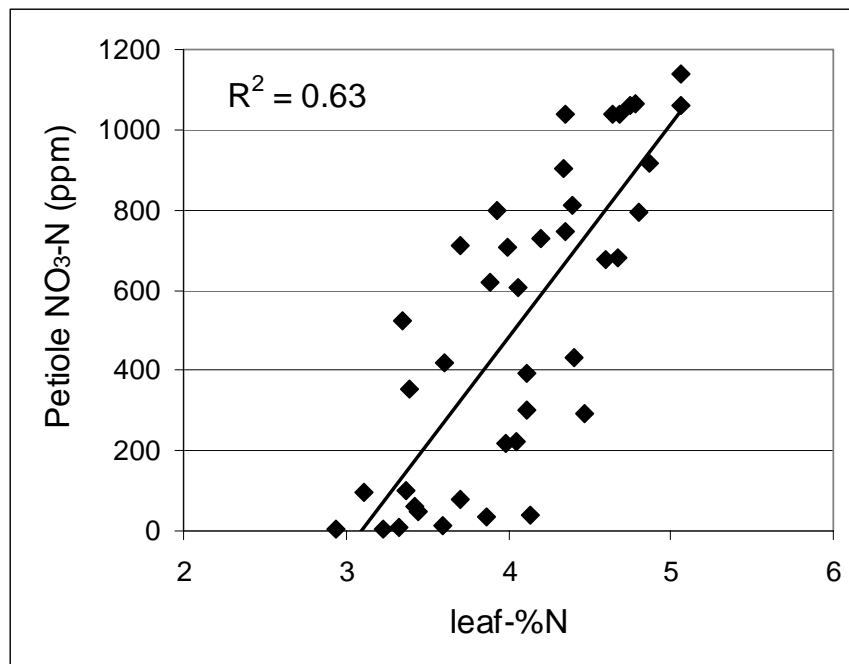


Figure 11: Leaf-%N against petiole $\text{NO}_3\text{-N}$ (data from 2007)

Our future research will investigate aerial HS images and assess the correlation of simulated $\text{VEN}\mu\text{S}$ images (rather than bands only) with spatial variability of N levels in potato fields. If aerial HS images and /or simulated $\text{VEN}\mu\text{S}$ satellite images should be found to be highly correlated with the spatial variability of leaf-%N and not with petiole

NO₃-N then additional research would be required to relate petiole NO₃-N content to leaf-%N or the leaf-%N to N fertilization decisions.

Acknowledgements

This project was supported by the Israeli Space Agency, Israeli Ministry of Science. And also by Research Grant Award No. CA-9102-06 from BARD-AAFC - The United States - Israel Binational Agricultural Research and Development Fund and Agriculture and Agri-Food, Canada.

The authors wish to express their appreciation of the vital contributions of Gadi Hadar and Ran Ferdman, potato growers from Kibbutz Ruhama, who provided land, seed and pesticide, and managed the irrigation for the project at no cost. The field experiments could not have been performed without the collaboration of Yossi Sofer, of Haifa Chemicals, Ltd.

References

- Al-Abbas, A.H., Barr, R., Hall, J.D., Crane, F.L., & Baumgardner, M.F. (1974). Spectra of normal and nutrient-deficient maize leaves. *Agronomy Journal*, 66, 16–20.
- Alchanatis, V., Schmilovitch, Z., & M. Meron (2005). In-field assessment of single leaf nitrogen status by spectral reflectance measurements. *Precision Agriculture*, 6, 25-39.

- Alva, K. A., (2008). Water management and water uptake efficiency by potatoes: A review. *Archives of Agronomy and Soil Science*, 54, 53–68.
- Bonfil D. J., Karnieli, A., Raz, M., Mufradi, I., Asido, S., Egozi, H., Hoffman, A., & Schmilovitch, Z. (2005). Rapid assessing of water and nitrogen status in wheat flag leaves. *Journal of Food Agriculture and Environment*, 3, 148-153.
- Botha, E. J., Zebarth, B. J., & Leblon, B. (2006). Non-destructive estimation of potato leaf chlorophyll and protein contents from hyperspectral measurements using the PROSPECT radiative transfer model. *Canadian Journal of Plant Science*, 86, 279–291.
- Coops, N. C., Smith, M.L., Martin, M. E., & Ollinger, S. V. (2003). Prediction of eucalypt foliage nitrogen content from satellite-derived hyperspectral data. *IEEE Transactions on Geoscience and Remote Sensing*, 41, 1338-1346.
- Dar, Z., (2002). *Potato crop protocol*. Ministry of Agriculture Extension Service, Bet Dagan, Israel. (in Hebrew).
- Daughtry, C. S. T., Walthall, C. L., Kim, M. S., Brown de Colstoun E., & McMurtrey, J. E. (2000). Estimating corn leaf chlorophyll concentration from leaf and canopy reflectance. *Remote Sensing of the Environment*, 74, 229–239.
- Errebhi, M., Rosen, C. J., Gupta, S. C., & Birong, D. E. (1998). Potato yield response and nitrate leaching as influenced by nitrogen management. *Agronomy Journal*, 90, 10–15.

- Ferguson, R. B., Hergert, G. W., Schepers, J. S., Gotway, C. A., Cahoon, J. E., & Peterson, T. A. (2002). Site-specific nitrogen management of irrigated maize: yield and soil residual nitrate effects. *Soil Science Society of America Journal*, 66, 544–553.
- Gates, D. M., Keegan, H. J., Schleter, J. C., & Weidner, V. R. (1965). Spectral properties of plants. *Applied Optics*, 4, 11–20.
- Gitelson, A. A., & Merzlyak, M. N. (1998). Remote sensing of chlorophyll concentration in higher plant leaves. *Advances in Space Research*, 22, 689–692.
- Gitelson, A. A., Gritz, Y., & Merzlyak, M. N. (2003). Relationships between leaf chlorophyll content and spectral reflectance and algorithms for non-destructive chlorophyll assessment in higher plant leaves. *Journal of Plant Physiology*, 160, 270–282.
- Haboudane, D., Miller, J. R., Tremblay, N., Zarco-Tejada, P. J., Dextraze, L. (2002). Integrated narrow-band vegetation indices for prediction of crop chlorophyll content for application to precision agriculture. *Remote Sensing of Environment*, 81, 416–426.
- Haboudane, D., Miller, J. R., Pattey, E., Zarco-Tejada, P. J., & Strachan, I. B. (2004). Hyperspectral vegetation indices and novel algorithms for predicting green LAI of crop canopies: Modeling and validation in the context of precision agriculture. *Remote Sensing of Environment*, 90, 337–352.
- Hu, B. X., Qian, S. E., Haboudane, D., Miller, J. R., Hollinger, A. B., Tremblay, N., & Pattey, E. (2004). Retrieval of crop chlorophyll content and leaf area index from decompressed hyperspectral data: the effects of data compression. *Remote Sensing of Environment*, 92, 139–152.

- Jain, N., Ray, S. S., Singh, J. P., & Panigrahy, S. (2007). Use of hyperspectral data to assess the effects of different nitrogen applications on a potato crop. *Precision Agriculture*, 8, 225–239.
- Meyer, R. D., & Marcum, D. B. (1998). Potato yield, petiole nitrogen, and soil nitrogen response to water and nitrogen. *Agronomy Journal*, 90, 420–429.
- National Potato Council (NPC). (2006). *Potato statistical yearbook, 2006–2007*. National Potato Council, Washington, DC. 82 pp.
- Ollinger, S. V., Smith, M. L., Martin, M. E., Hallett, R. A., Goodale, C. L., & Aber, J. D. (2002). Regional variation in foliar chemistry and N cycling among forests of diverse history and composition. *Ecology*, 83, 339–355.
- Shenk, J. & Westerhaus, M. (1991). Population structuring of near infrared spectra and modified partial least squares regression, *Crop Science*, 31, 1548–1555.
- Shock, C. C., Pereira, A. B., & Eldredge, E. B. (2007). Irrigation best management practices for potato. *American Journal of Potato Research*, 84, 29–37.
- Smith, M. L., Ollinger, S. V., Martin, M. E., Aber, J. D., Hallett, R. A., & Goodale, C. L. (2002). Direct estimation of aboveground forest productivity through hyperspectral remote sensing of canopy nitrogen. *Ecological Applications*, 12, 1286–1302.
- Strachan, I. B., Pattey, E., & Boisvert, J. B. (2002). Impact of nitrogen and environmental conditions on corn as detected by hyperspectral reflectance. *Remote Sensing of Environment* 80, 213–224.

- Thomas, J. R., & Gausman, H. W. (1977). Leaf reflectance vs. leaf chlorophyll and carotenoid concentrations for eight crops. *Agronomy Journal* 69, 799–802.
- Townsend, P. A., Foster, J. R., Chastain, R. A., & Currie, W. S. (2003). Application of imaging spectroscopy to mapping canopy nitrogen in the forests of the central Appalachian Mountains using Hyperion and AVIRIS. *IEEE Transactions on Geoscience and Remote Sensing*, 41, 1347-1354.
- Tso, B., & Mather, P. (2001). *Classification methods for remote sensed data*. CRC, Boca Raton, FL. 356 pp.
- Van-Alphen, B. J., & Stoorvogel, J. J. (2000). A functional approach to soil characterization in support of precision agriculture. *Soil Science Society of American Journal*, 64, 1706-1713.
- Westermann, D. T., & Kleinkopf, G.E. (1985). Nitrogen requirements of potatoes. *Agronomy Journal* 77, 616-621.
- Zakaluk, R., & Ranjan, R. S. (2007). Artificial neural network modelling of leaf water potential for potatoes using RGB digital images: a greenhouse study. *Potato Research*, 49, 255-272.
- Zarco-Tejada, P. J., Berjon, A., Lopez-Lozano, R., Miller, J. R., Martin, P., Cachorro, V., Gonzalez, M. R., & de Frutos, A. (2005), Assessing vineyard condition with hyperspectral indices: leaf and canopy reflectance simulation in a row-structured discontinuous canopy. *Remote Sensing of Environment*, 99, 271-287.

Zebarth, B. J., & Rosen, C. J. (2007). Research perspective on nitrogen BMP development for potato. *American Journal of Potato Research*, 84, 3-18.